# Vorticity-induced anomalous Hall effect in an electron fluid

Hiroshi Funaki,[1,2] Riki Toshio,[3] and Gen Tatara[1,2]
[1]*RIKEN Center for Emergent Matter Science (CEMS), 2-1 Hirosawa, Wako, Saitama, 351-0198, Japan*
[2]*RIKEN Cluster for Pioneering Research (CPR), 2-1 Hirosawa, Wako, Saitama, 351-0198, Japan*
[3]*Department of Physics, Kyoto University, Kyoto 606-8502, Japan*

(Received 2 March 2021; revised 1 June 2021; accepted 8 July 2021; published 21 July 2021)

We develop a hydrodynamic theory for an electron system exhibiting the anomalous Hall effect, and show that an additional anomalous Hall effect is induced by a vorticity generated near boundaries. We calculate the momentum flux and force proportional to the electric field using linear response theory. The hydrodynamic equation is obtained by replacing the local electric field with the electric current, focusing on a scale that is sufficiently larger than the mean-free path. It is demonstrated that there is a coupling between a vorticity of an electric current and a magnetization which generates a pressure from nonuniform vorticity. Taking into account Hall viscosity and relaxation forces, a nonuniform flow near a boundary and an additional Hall force are calculated. The additional anomalous Hall force is opposite to a conventional anomalous Hall force, resulting in a sign reversal in thin systems. An antisymmetric viscosity turns out to arise from the side-jump process due to the anomalous velocity.

DOI: 10.1103/PhysRevResearch.3.033075

## I. INTRODUCTION

Spin, a form of angular momentum, leads to various exotic phenomena different from those of charge. A typical example is spin-rotational coupling, where the angular momentum of mechanical rotation couples directly to spin, inducing the classical Einstein-de Haas effect. Spin-rotation coupling was derived from the Dirac equation in a rotating frame in Ref. [1]. A spin-vorticity coupling to the vorticity of the electron flow, $\boldsymbol{\omega} = \nabla \times \boldsymbol{j}_{\rm e}$, where $\boldsymbol{j}_{\rm e}$ is the electron current density, was derived and spin current generation was discussed recently [2]. Spin vorticity coupling is natural from the view point of the Faraday's law, $\dot{\boldsymbol{B}} = -\nabla \times \boldsymbol{E}$ between electric and magnetic fields, $\boldsymbol{E}$ and $\boldsymbol{B}$, respectively. In fact, the right-hand side is proportional to the vorticity of electric current, as local electric current density is related in the linear response regime to the electric field as $\boldsymbol{j}_{\rm e} = \sigma_{\rm e}\boldsymbol{E}$, where $\sigma_{\rm e}$ is the electric conductivity and spin density is induced by a magnetic field.

Spin Hall effect, where spin density [3] and current [4] are induced by an applied electric field, recently turned out to be interpreted as due to the spin-vorticity coupling [5]. It was shown there that the induced spin density $\boldsymbol{s}$ in the ballistic regime is written as $\boldsymbol{s} = \lambda_{\rm sh}(\nabla \times \boldsymbol{j}_{\rm e})$, where $\lambda_{\rm sh}$ is a constant arising from the spin-orbit interaction, indicating an effective spin-vorticity coupling of the form $\boldsymbol{s} \cdot \boldsymbol{\omega}$. (In the diffusive case, the coupling exists but becomes nonlocal due to diffusion.) As expected from the symmetry and Faraday's law, $\lambda_{\rm sh}$ is proportional to the electron relaxation time $\tau$, meaning that relaxation is essential for the development of spin density. The above studies indicate that spin-vorticity coupling, arising as a natural consequence of the spin-orbit interaction, is a fundamental coupling for various spintronics effects.

Spin-vorticity coupling suggests that there is also a magnetization-vorticity coupling inducing a rotational motion due to a magnetization in ferromagnets. The aim of the present paper is to demonstrate that such a coupling indeed emerges as a result of an anomalous Hall (AH) effect. Vorticity of electrons in solids has not been discussed in the context of conventional electron transport properties focusing on the spatially averaged responses. In mesoscopic systems and interface/surface transports, in contrast, vorticity of flow in the meso or macroscopic size would be crucially important. Hydrodynamic description, which integrates out microscopic features, become a powerful tool to take account of such vortical effects. In fact, recent intense studies of *electron hydrodynamics*, which is quickly growing into a mature field of condensed matter physics today [6,7], has predicted and demonstrated various unconventional transport phenomena driven by vorticity or a velocity gradient, including negative local resistance [8–11], anomalous viscous magnetotransport [12–17], spin hydrodynamic generation [18], generalized vortical effect [19,20], and chiral angular momentum generation [21]. In this paper, we choose a hydrodynamic approach for the analysis of the Ohmic fluid in AH systems and evaluate the momentum flux density based on a microscopic linear response theory, as done in Ref. [21]. Considering low temperatures, the effects of magnons are neglected.

Spin is an axial vector breaking the time-reversal symmetry, and thus the hydrodynamic coefficients are modified when an internal spin degrees of freedom is taken account [22,23]. As for conventional fluid, spin corresponds to a rotation of each molecule, while it is the electron's quantum mechanical spin in the case of our electron fluid, but they are equivalent from the viewpoint of symmetry. A hydrodynamic equation taking account of spin explicitly was discussed on a phenomenological basis by Snider and Lewchuk [23]. It was argued that momentum flux density tensor, $\pi_{ij}$, which is even under both spatial inversion and time-reversal, may have a term linear in spin, $\boldsymbol{s}$, if there is an external magnetic field $H$ (or magnetization $M$) or vorticity of fluid $\omega = \nabla \times \boldsymbol{j}_{\rm e}$. The diagonal term of $\pi_{ij}$ describing pressure therefore has a spin-vorticity coupling proportional to $\boldsymbol{s}\cdot\boldsymbol{\omega}$ argued later microscopically in Ref. [1,2]. Considering a ferromagnetic electron fluid, electron spin is polarized along the magnetization $\boldsymbol{M}$, i.e., $\boldsymbol{s} \propto \boldsymbol{M}$, and thus the spin-vorticity coupling identified in Ref. [23] reduces to a spin-magnetization coupling $\boldsymbol{M}\cdot\boldsymbol{\omega}$ when electron spin is traced out. Our microscopic study turns out to justify this phenomenological argument and, moreover, it provides an explicit expression describing the magnitude of the magnetization-vorticity coupling.

## II. ANOMALOUS HALL ELECTRON FLUID

Electrons in solids are dense and are regarded as a continuum medium or a fluid. Macroscopic or mesoscopic transport properties of electron fluid are characterized by the forces acting on the fluid. Besides external forces, such as the one due to the electric field and the Lorentz force, there are viscosity forces and relaxation forces induced by internal interactions and scatterings [21,24]. The viscosity force arising from inhomogeneity of fluid velocity is larger for longer relaxation times (weaker relaxation), as the relaxation effects cut off interaction effects that lead to viscosity. In most metals with disorder, the steady electron transport is determined by a relaxation force. The force is opposite to the fluid velocity and is written as $\boldsymbol{f}_{\rm r} = -m\boldsymbol{j}/\tau$, where $m$ is the electron mass, $\tau$ is the total relaxation time, and $\boldsymbol{j}$ is the current density without the electron charge $e$ ($e\boldsymbol{j} = \boldsymbol{j}_{\rm e}$). Depending on the relaxation time, therefore, electron fluids are classified into two regimes, a viscous fluid and Ohmic fluid, where viscosity and relaxation dominates, respectively. Most metals are in the Ohmic regime, while viscous fluids have been realized recently in extremely clean systems such as graphene [7,9,17,25–27], GaAs quantum wells [28,29], 2D monovalent layered metal $PdCoO_2$ [15], and various semimetallic materials including $WP_2$ [16], $WTe_2$ [30], MoP [31], Sb [32], and $ZrTe_5$ [33].

Here we study an electron fluid showing AH effect due to a uniform magnetization $\boldsymbol{M}$. The systems we have in mind are ordinary ferromagnets such as Fe and Co, and thin metals and semiconductors under an external magnetic field. Considering the Ohmic regime, we take account of a spin-orbit interaction arising from impurities, on the same footing as the studies of AH conductivity [34]. Calculating the momentum flux density within the linear response theory, we show that the AH liquid has a magnetization-vorticity coupling, $\boldsymbol{M}\cdot\boldsymbol{\omega}$, besides an anomalous viscosity argued previously [13]. The magnetization-vorticity coupling is a spin-polarized counterpart of the spin-vorticity coupling. In terms of the force density, the contribution reads $\tilde{\lambda}\nabla(\hat{\boldsymbol{M}}\cdot\boldsymbol{\omega})$ with a coefficient $\tilde{\lambda}$. In the case of a thin film ferromagnet with an in-plane magnetization with an applied electric field, this coupling induces a voltage perpendicular to the magnetization and the applied electric field. The direction of the output voltage is opposite to the conventional bulk AH effect. The reduction of Hall effect due to a Hall viscosity was reported in Ref. [13]. We also identify an AH force $f_{\rm AH}(\hat{\boldsymbol{M}}\times\boldsymbol{j})$ ($f_{\rm AH}$ is a coefficient and $\hat{\boldsymbol{M}} \equiv \boldsymbol{M}/M$), which is analogous to the Lorentz force. The total force density acting on the AH fluid with uniform and steady flow is therefore $\boldsymbol{f} = en\boldsymbol{E} - \frac{m}{\tau}\boldsymbol{j} + f_{\rm AH}(\hat{\boldsymbol{M}}\times\boldsymbol{j})$. When an electric field $\boldsymbol{E}$ is perpendicular to the magnetization, the steady flow realized is $e\boldsymbol{j} = \sigma_{\rm e}E + \sigma_{\rm ah}(\hat{\boldsymbol{M}}\times\boldsymbol{E})$ with $\sigma_{\rm AH}/\sigma_{\rm e} = \frac{\tau}{m}f_{\rm AH}$ to the lowest order in the spin-orbit interaction.

The magnetization-vorticity coupling found here is in the diagonal part of the momentum flux density, $\pi_{ij}$, presenting a potential for the electron, and thus does not generate angular momentum. In fact, the magnetization-vorticity coupling induces a pressure $\boldsymbol{f}_{\boldsymbol{\omega}} = \tilde{\lambda}\nabla(\boldsymbol{\omega}\cdot\boldsymbol{M})$, and its contribution to the orbital angular momentum vanishes, as $\int d^3r[\boldsymbol{r}\times\nabla(\boldsymbol{\omega}\cdot\boldsymbol{M})] = 0$ if we use integral by parts. This is because the coupling is between two angular momenta and thus linear velocity does not generate angular momentum. In contrast, in chiral systems, an angular momentum couples to a linear momentum, resulting in an angular momentum generation by a linear momentum [19,21].

Besides the magnetization-vorticity coupling, another unique feature of the present system is the existence of the antisymmetric components $\pi^{\rm a}_{ij}$ ($= -\pi^{\rm a}_{ji}$) of the momentum flux density, which is peculiar to the fluids with internal angular momentum. It is written generally as $\pi^{\rm a}_{ij} = \epsilon_{ijk}a_k$, where $\boldsymbol{a}$ is a vector even in the space inversion (axial vector), because $\pi_{ij}$ is even. Hence, from the symmetry viewpoint, $\pi^{\rm a}_{ij}$ is expected to arise from spin and vorticity as argued phenomenologically [22,23,35]. We demonstrate that the present AH system in fact has the antisymmetric components $\pi^{\rm a}_{ij}$ arising from the side-jump process due to the anomalous velocity. Our results are consistent with phenomenological argument of Ref. [23]. Although the side-jump process in disordered metals is smaller than the skew-scattering contribution by a factor of $(\epsilon_F\tau)^{-1/2}$, where $\epsilon_F$ is the Fermi energy, the observation of the antisymmetric viscosity in an AH electron system is therefore regarded as a confirmation of the existence of anomalous velocity and the side-jump mechanism.

Moreover, the anomalous velocity of the quantum system gives rise to an interesting possibility of different hydrodynamic equations depending on the descriptions based on velocity or momentum. While they are proportional to each other for classical particles, they are not when an anomalous velocity exists due to interactions. In this paper, we consider the hydrodynamic equation for momentum density, as its time-derivative is a force, which is observable. The two choices are, however, equivalent if calculated correctly.

## III. FORMALISM

The model we consider is a conduction electron with a spin polarization due to a uniform localized spin (magnetization) $\boldsymbol{S}$ and spin-orbit interaction. The Hamiltonian for the electron is

$H \equiv H_K + H_M + H_{so} + H_i$, where

$$H_K = \int d^3 r c^\dagger \frac{-\nabla^2}{2m} c \tag{1}$$

is the kinetic part, and

$$H_M \equiv -\sum_{\boldsymbol{k}} c_{\boldsymbol{k}}^\dagger (\boldsymbol{M}\cdot\boldsymbol{\sigma}) c_{\boldsymbol{k}} \tag{2}$$

is the exchange interaction to the magnetization, where $\boldsymbol{M} \equiv J\boldsymbol{S}$ with $J$ being a coupling constant. The spin-orbit interaction is the one arising from random impurities, represented by a Hamiltonian

$$\begin{aligned} H_{so} &= \lambda_{so} \int d^3 r c^\dagger(\boldsymbol{r})[(\nabla u_i(\boldsymbol{r}) \times \hat{\boldsymbol{p}})\cdot\boldsymbol{\sigma}]c(\boldsymbol{r}) \\ &= i\lambda_{so} \sum_{\boldsymbol{k}\boldsymbol{k}'} u_{\boldsymbol{k}'-\boldsymbol{k}} (\boldsymbol{k}' \times \boldsymbol{k}) \cdot c_{\boldsymbol{k}'}^\dagger \boldsymbol{\sigma} c_{\boldsymbol{k}}, \end{aligned} \tag{3}$$

where $u_i(\boldsymbol{r}) = u_i \sum_{\boldsymbol{R}_i} \delta(\boldsymbol{r}-\boldsymbol{R}_i)$ is an impurity potential, where $u_i$ is the strength of the impurity potential, and $\boldsymbol{R}_i$ is the position of $i$th impurity. $u_{\boldsymbol{k}'-\boldsymbol{k}} = u_i \sum_{\boldsymbol{R}_i} e^{-i(\boldsymbol{k}'-\boldsymbol{k})\cdot\boldsymbol{R}_i}$ is the Fourier transform of the impurity potential. The spin-orbit interaction leads to a correction to the electric velocity operator (anomalous velocity):

$$\delta \boldsymbol{v}(\boldsymbol{r}) = -i\lambda_{so} \sum_{\boldsymbol{k}\boldsymbol{k}'\boldsymbol{q}} u_{\boldsymbol{q}} e^{i(\boldsymbol{k}-\boldsymbol{k}'+\boldsymbol{q})\cdot\boldsymbol{r}} c_{\boldsymbol{k}'}^\dagger (\boldsymbol{q}\times\boldsymbol{\sigma}) c_{\boldsymbol{k}}. \tag{4}$$

Considering the diffusive (Ohmic) regime, an impurity scattering Hamiltonian,

$$H_i = \sum_{\boldsymbol{k}\boldsymbol{k}'} u_{\boldsymbol{k}'-\boldsymbol{k}} c_{\boldsymbol{k}'}^\dagger c_{\boldsymbol{k}}, \tag{5}$$

is included. The elastic lifetime arising from the impurity scattering, $\tau_e$, is given by $\tau_e^{-1} = 2\pi\nu u_i^2 n_i$, where $\nu$ and $n_i$ are density of states and impurity concentration, respectively. We treat it as spin independent to simplify the calculation.

We study the effects of the AH effect on the hydrodynamic behaviors of the electron, taking account both the spin-orbit interaction and an applied electric field to the linear order. A hydrodynamic equation is derived by calculating the equation of motion for the momentum density, $\boldsymbol{p} \equiv \langle c^\dagger \hat{\boldsymbol{p}} c\rangle$ ($\hat{\boldsymbol{p}} \equiv -i\nabla$ is the momentum operator) by use of the Heisenberg equation of motion, $\dot{\boldsymbol{p}} = i[H, c^\dagger \hat{\boldsymbol{p}} c]$. The commutator with the kinetic part is

$$i[H_K, c^\dagger \hat{p}_i c] = -\nabla_j \pi_{ij}^0, \tag{6}$$

where the momentum flux density contribution is

$$\pi_{ij}^0(\boldsymbol{r},t) = -i\frac{1}{m}\mathrm{tr}[\hat{p}_i\hat{p}_j G^<(\boldsymbol{r},t,\boldsymbol{r},t)], \tag{7}$$

with $G^<(\boldsymbol{r},t,\boldsymbol{r}',t') = i\langle c^\dagger(\boldsymbol{r}',t')c(\boldsymbol{r},t)\rangle$ being the lesser Green's function and tr is the summation over spin. The spin-orbit contribution is

$$i[H_{so}, c^\dagger \hat{p}_i c] = -\nabla_j \pi_{ij}^{so} + f_i^{so}, \tag{8}$$

where the momentum flux density contribution from the spin-orbit interaction is (see Appendix B)

$$\begin{aligned} \pi_{ij}^{so}(\boldsymbol{r},t) = \frac{\lambda_{so}}{2}\epsilon_{jkl}(\nabla_k u_i(\boldsymbol{r}))\left(\nabla_i^{\boldsymbol{r}} - \nabla_i^{\boldsymbol{r}'}\right) \\ \times\ \mathrm{tr}[\sigma_l G^<(\boldsymbol{r},t,\boldsymbol{r}',t)]|_{\boldsymbol{r}'\to\boldsymbol{r}}, \end{aligned} \tag{9}$$

where $\epsilon_{jkl}$ is the Levi-Civita symbol. The term $f_i^{so}$ is a contribution not written as a divergence, which is

$$\begin{aligned} f_i^{so}(\boldsymbol{r},t) = -\frac{\lambda_{so}}{2}\epsilon_{jkl}(\nabla_i\nabla_j u_i(\boldsymbol{r}))\left(\nabla_k^{\boldsymbol{r}} - \nabla_k^{\boldsymbol{r}'}\right) \\ \times\ \mathrm{tr}[\sigma_l G^<(\boldsymbol{r},t,\boldsymbol{r}',t)]|_{\boldsymbol{r}'\to\boldsymbol{r}}. \end{aligned} \tag{10}$$

The impurity contribution leads to a force:

$$f_i^{i} = -i(\nabla_i u_i)\mathrm{tr}[G^<(\boldsymbol{r},t,\boldsymbol{r},t)]. \tag{11}$$

The hydrodynamic equation of the present system is therefore\vskip3pt

$$\dot{p}_i = -\nabla_j \pi_{ij} + f_i^{so} + f_i^{i}, \tag{12}$$

where the momentum flux density is

$$\begin{aligned} \pi_{ij} &= \pi_{ij}^0 + \pi_{ij}^{so} \\ &= -i\mathrm{tr}[\hat{p}_i\hat{v}_j G^<(\boldsymbol{r},t,\boldsymbol{r},t)], \end{aligned} \tag{13}$$

where $\hat{v} \equiv \frac{\hat{\boldsymbol{p}}}{m} + \hat{\delta\boldsymbol{v}}$ is the total velocity operator and $\pi_{ij}^0$ is the normal contribution without spin-orbit interaction. Since $\hat{v}$ includes $\hat{\delta\boldsymbol{v}}$, $\pi_{ij}$ has antisymmetric components.

## IV. DERIVATION OF HYDRODYNAMIC EQUATION

The momentum flux density $\pi_{ij}$ is calculated in the presence of a driving field, an applied static electric field $\boldsymbol{E}$. In the linear response theory, we have $\pi_{ij} = \pi_{ijk} e E_k$, where $\pi_{ijk}$ is the correlation function of $\hat{p}_i\hat{v}_j$ and $\hat{v}_k$. The calculation of the response function is parallel to that of the AH conductivity $\sigma_{xy}$ in Ref. [34]. There are two processes, one arising from the normal velocity $\frac{\hat{\boldsymbol{p}}}{m}$, the contribution historically called skew-scattering contribution, and the other arising from the anomalous velocity $\hat{\delta\boldsymbol{v}}$, called the side-jump contribution. The dominant contribution at dilute impurity concentration turns out to be the skew scattering one containing impurity scattering to the second order besides the spin-orbit interaction [34], diagrammatically depicted in Fig. 1(a). The processes with less impurity shown in Fig. 1(b) vanish as the factor of $\boldsymbol{k}'\times\boldsymbol{k}$ in the spin-orbit interaction changes signs for the two conjugate processes. The skew-scattering contribution is thus (ss denotes skew-scattering, and $V$ is the system volume)

$$\begin{aligned} \pi_{ijk}^{ss}(\boldsymbol{q}) = \frac{1}{2\pi V^3}\frac{i\lambda_{so}u_i^3 n_i}{m^2}\sum_{\boldsymbol{k}\boldsymbol{k}'\boldsymbol{k}''} k_i k_j k'_k \left[\left(\boldsymbol{k}' - \frac{\boldsymbol{q}}{2}\right)\times\left(\boldsymbol{k} - \frac{\boldsymbol{q}}{2}\right)\right]_l \\ \times\ 2\mathrm{Re}\mathrm{tr}\left[\sigma_l G^r_{\boldsymbol{k}+\frac{\boldsymbol{q}}{2}} G^r_{\boldsymbol{k}'+\frac{\boldsymbol{q}}{2}} G^a_{\boldsymbol{k}'-\frac{\boldsymbol{q}}{2}} G^a_{\boldsymbol{k}-\frac{\boldsymbol{q}}{2}} G^r_{\boldsymbol{k}''}\right], \end{aligned} \tag{14}$$

where $G^r_{\boldsymbol{k}} \equiv [-\frac{k^2}{2m} + \boldsymbol{M}\cdot\boldsymbol{\sigma} + \frac{i}{2\tau_e}]^{-1}$ is the retarded Green's function with elastic lifetime $\tau_e$ and $G^a_{\boldsymbol{k}} \equiv (G^r_{\boldsymbol{k}})^*$. We choose $\boldsymbol{M}$ along the $z$ axis and calculate the response function to the lowest order in the external wave vector $\boldsymbol{q}$. Summation

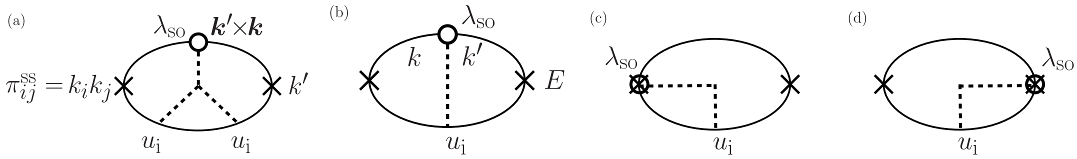


FIG. 1. Feynman diagrams for the dominant contribution to the momentum flux density at the linear order in the spin-orbit interaction and linear response to the applied field, denoted by $\times$ at the right end. Solid lines represent electron Green's functions, where upper and lower lines denote retarded and advanced Green's functions, respectively, and $\boldsymbol{k}$ and $\boldsymbol{k}'$ are the electron wave vectors. Complex conjugate processes (turned upside down) are also taken into account. (a) The dominant contribution (skew scattering). The left vertex with $k_ik_j$ represents the vertex for the momentum flux density and a vertex with $\lambda$ denotes the spin-orbit interaction. (b) The contribution that vanishes when a complex conjugate process (upside-down) is summed. (c), (d) The contributions arising from the anomalous velocity $\delta v$, called the side-jump contributions. The process (c) gives rise to an antisymmetric component of the flux density. The contributions are smaller than the one in (a) by a factor of $(\epsilon_F\tau_{\mathrm{e}})^{-1/2}$.

over the wave vectors are carried out as

$$\frac{1}{V}\sum_{\boldsymbol{k}} G^{\mathrm{a}}_{\boldsymbol{k}} = i\pi\nu, \quad \frac{1}{V}\sum_{\boldsymbol{k}} k_ik_jG^{\mathrm{r}}_{\boldsymbol{k}}G^{\mathrm{a}}_{\boldsymbol{k}} = \frac{2\pi}{3}\nu {k_F}^2\tau_{\mathrm{e}}\delta_{ij}$$

$$\frac{1}{V}\sum_{\boldsymbol{k}} k_ik_jk_kG^{\mathrm{r}}_{\boldsymbol{k}+\frac{\boldsymbol{q}}{2}}G^{\mathrm{a}}_{\boldsymbol{k}-\frac{\boldsymbol{q}}{2}} = -i\frac{2\pi}{15m}\nu {k_F}^4\tau_{\mathrm{e}}^2(\delta_{ij}q_k+\delta_{ik}q_j+\delta_{jk}q_i), \tag{15}$$

where $\nu$ and $k_F$ are the spin-dependent density of states and Fermi wave vector, respectively. The result is

$$\pi^{\mathrm{ss}}_{ijk}(\boldsymbol{q}) = i\lambda(\delta_{ij}\epsilon_{lkz}q_l+\epsilon_{ikz}q_j+\epsilon_{jkz}q_i), \tag{16}$$

where the coefficient is ($\pm$ denotes the direction of spin along the $z$ axis)

$$\lambda \equiv \frac{4\pi^2}{45}\frac{\lambda_{\mathrm{so}}u_{\mathrm{i}}^3n_{\mathrm{i}}}{m^3}\sum_{\pm}(\pm)(\nu_\pm)^3(k_{\mathrm{F}\pm})^6\tau_{\mathrm{e}}^3. \tag{17}$$

The contribution vanishes if there is no spin polarization ($M=0$).

The contributions arising from the anomalous velocity $\delta\boldsymbol{v}$ [the side-jump contributions, depicted in Figs. 1(c) and 1(d)] are

$$\pi^{\mathrm{sj(c)}}_{ijk}(\boldsymbol{q}) = \frac{-i}{2\pi V^2}\frac{\lambda_{\mathrm{so}}u_{\mathrm{i}}^2n_{\mathrm{i}}}{2m}\epsilon_{jlz}\sum_{\boldsymbol{k}\boldsymbol{k}'}\frac{(k'+k+q)_i}{2}\left(k+\frac{q}{2}\right)_k(k'-k)_l 2\mathrm{Re}\mathrm{tr}\left[\sigma_zG^{\mathrm{r}}_{\boldsymbol{k}'}G^{\mathrm{r}}_{\boldsymbol{k}}G^{\mathrm{a}}_{\boldsymbol{k}+\boldsymbol{q}}\right],$$

$$\pi^{\mathrm{sj(d)}}_{ijk}(\boldsymbol{q}) = \frac{-i}{2\pi V^2}\frac{\lambda_{\mathrm{so}}u_{\mathrm{i}}^2n_{\mathrm{i}}}{2m}\epsilon_{klz}\sum_{\boldsymbol{k}\boldsymbol{k}'}\left(k+\frac{q}{2}\right)_i\left(k+\frac{q}{2}\right)_j(k'-k)_l 2\mathrm{Re}\mathrm{tr}\left[\sigma_zG^{\mathrm{r}}_{\boldsymbol{k}'}G^{\mathrm{r}}_{\boldsymbol{k}}G^{\mathrm{a}}_{\boldsymbol{k}+\boldsymbol{q}}\right], \tag{18}$$

which turn out to be

$$\pi^{\mathrm{sj(c)}}_{ijk}(\boldsymbol{q}) = i\eta^{\mathrm{sj}}\left(-\frac{2}{3}\epsilon_{jiz}q_k+\delta_{ik}\epsilon_{jlz}q_l+\epsilon_{jkz}q_l\right),$$

$$\pi^{\mathrm{sj(d)}}_{ijk}(\boldsymbol{q}) = i\eta^{\mathrm{sj}}2(\delta_{ij}\epsilon_{klz}q_l-\epsilon_{ikz}q_j-\epsilon_{jkz}q_i), \tag{19}$$

where

$$\eta^{\mathrm{sj}} \equiv \frac{\pi}{15}\frac{\lambda_{\mathrm{so}}u_{\mathrm{i}}^2n_{\mathrm{i}}}{m^2}\sum_{\pm}(\pm)(\nu_\pm)^2k_{\mathrm{F}\pm}^4\tau_{\mathrm{e}}^2. \tag{20}$$

The total side-jump contribution $\pi^{\mathrm{sj}}_{ijk}\equiv\pi^{\mathrm{sj(c)}}_{ijk}+\pi^{\mathrm{sj(d)}}_{ijk}$ is

$$\pi^{\mathrm{sj}}_{ijk}(\boldsymbol{q}) = i\eta^{\mathrm{sj}}\left(-\frac{2}{3}\epsilon_{jiz}q_k+\delta_{ik}\epsilon_{jlz}q_l+2\delta_{ij}\epsilon_{klz}q_l-2\epsilon_{ikz}q_j-\epsilon_{jkz}q_i\right). \tag{21}$$

The side-jump contribution has a unique contribution asymmetric with respect to $i$ and $j$, although the magnitude proportional to $u_{\mathrm{i}}^2\tau_{\mathrm{e}}^2$ is smaller than the skew scattering one by a factor of $(\epsilon_F\tau_{\mathrm{e}})^{-1/2}$ (noting that $u_{\mathrm{i}}\propto{\tau_{\mathrm{e}}}^{-1/2}$). The contribution to the spin-orbit induced momentum flux density $\pi^{\mathrm{so}}_{ij}=\pi^{\mathrm{ss}}_{ij}+\pi^{\mathrm{sj}}_{ij}$ is therefore

$$\begin{aligned}\frac{1}{e}\pi^{\mathrm{so}}_{ij}(\boldsymbol{r}) &= (\lambda-2\eta^{\mathrm{sj}})\delta_{ij}(\nabla\times\boldsymbol{E})\cdot\hat{\boldsymbol{M}}-\bar{\lambda}[\nabla_i(\hat{\boldsymbol{M}}\times\boldsymbol{E})_j+\nabla_j(\hat{\boldsymbol{M}}\times\boldsymbol{E})_i]\\ &\quad+\frac{2}{3}\eta^{\mathrm{sj}}\epsilon_{ijz}(\nabla\cdot\boldsymbol{E})-\frac{\eta^{\mathrm{sj}}}{2}[\nabla_i(\hat{\boldsymbol{M}}\times\boldsymbol{E})_j-\nabla_j(\hat{\boldsymbol{M}}\times\boldsymbol{E})_i]\\ &\quad-\eta^{\mathrm{sj}}(\hat{\boldsymbol{M}}\times\nabla)_jE_i,\end{aligned} \tag{22}$$

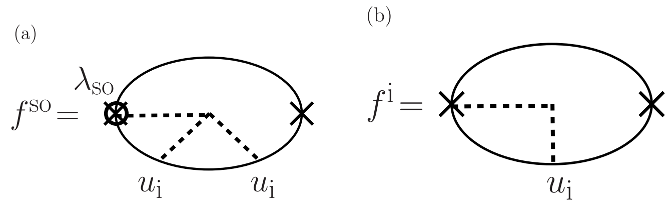


FIG. 2. Feynman diagrams for force due to (a) the spin-orbit interaction and (b) the impurities at the linear order at the linear response to the applied field.

where $\overline{\lambda} \equiv \lambda - 3\eta^{\mathrm{sj}}/2$ and $\hat{\boldsymbol{M}} \equiv \boldsymbol{M}/|\boldsymbol{M}|$ is chosen along $z$ axis. Here we see that an antisymmetric viscosity with respect to $i$ and $j$ arises from the side-jump process ($\eta^{\mathrm{sj}}$). The last term of Eq. (22) does not contribute to the hydrodynamic equation as $\nabla \cdot (\hat{\boldsymbol{M}} \times \nabla) = 0$.

Force densities are similarly calculated. The linear response contribution to a uniform component of the spin-orbit induced force density is $f_i^{\mathrm{so}} = f_{im}^{\mathrm{so}} E_m$, where (diagrammatically shown in Fig. 2)

$$f_{im}^{\mathrm{so}} \equiv \frac{1}{2\pi V^3} \frac{\lambda_{\mathrm{so}} u_{\mathrm{i}}^3 n_{\mathrm{i}}}{m} \sum_{\boldsymbol{k}\boldsymbol{k}'\boldsymbol{k}''} \epsilon_{jkl} (k'-k)_i (k'-k)_j (k'+k)_k k'_m 2\mathrm{Re}\mathrm{tr}\left[\sigma_l G_{\boldsymbol{k}}^{\mathrm{r}} G_{\boldsymbol{k}''}^{\mathrm{r}} G_{\boldsymbol{k}'}^{\mathrm{r}} G_{\boldsymbol{k}'}^{\mathrm{a}}\right]. \tag{23}$$

After summation over the wave vectors, we obtain $f_{im}^{\mathrm{so}} = -\epsilon_{imz} f_{\mathrm{AH}}$, with a coefficient

$$f_{\mathrm{AH}} = \frac{2\pi^2}{9} \frac{\lambda_{\mathrm{so}} u_{\mathrm{i}}^3 n_{\mathrm{i}}}{m} \sum_{\pm} (\pm) \nu_{\pm}^3 k_{\mathrm{F}\pm}^4 \tau_{\mathrm{e}}. \tag{24}$$

The force thus is the AH force:

$$\boldsymbol{f}^{\mathrm{so}} = -e f_{\mathrm{AH}} (\boldsymbol{E} \times \hat{\boldsymbol{M}}). \tag{25}$$

The relaxation force due to the impurities turns out to be $\boldsymbol{f}^{\mathrm{i}} = -en\boldsymbol{E}$, as was argued in Refs. [21,24].

Taking account of the normal viscosity $\pi_{ij}^0$ (calculated in Appendix A) and relaxation force, Eqs. (12), (22), and (25) describe the fluid as a response to the driving field $\boldsymbol{E}$. Conventional hydrodynamic equation, a relation between the momentum density and local velocity or current, is obtained by using $e\boldsymbol{j} = \sigma_{\mathrm{e}} \boldsymbol{E} + \sigma_{\mathrm{AH}} (\hat{\boldsymbol{M}} \times \boldsymbol{E})$, where $\sigma_{\mathrm{e}}$ and $\sigma_{\mathrm{AH}}$ are the longitudinal and AH conductivities, respectively. At the lowest order in the spin-orbit interaction, the hydrodynamic equation of the present system reads

$$\begin{aligned} \dot{\boldsymbol{p}} = {} & \tilde{\eta}_0 (2\nabla(\nabla \cdot \boldsymbol{j}) + \nabla^2 \boldsymbol{j}) - \tilde{\lambda}[\nabla[\nabla \cdot (\boldsymbol{j} \times \hat{\boldsymbol{M}})] + \nabla^2 (\boldsymbol{j} \times \hat{\boldsymbol{M}})] - \lambda_\omega \nabla(\boldsymbol{\omega} \cdot \hat{\boldsymbol{M}}) \\ & + \tilde{\eta}^{\mathrm{sj}} \left[\frac{2}{3} (\hat{\boldsymbol{M}} \times \nabla)(\nabla \cdot \boldsymbol{j}) + \frac{1}{2} [\nabla \times [\nabla \times (\hat{\boldsymbol{M}} \times \boldsymbol{j})]]\right] - \tilde{f}_{\mathrm{AH}} (\boldsymbol{j} \times \hat{\boldsymbol{M}}) - \frac{ne^2}{\sigma_{\mathrm{e}}} \boldsymbol{j} + en\boldsymbol{E}, \end{aligned} \tag{26}$$

where $\boldsymbol{\omega} \equiv \nabla \times \boldsymbol{j}$ is the vortex density, $\tilde{\lambda} = e^2 \overline{\lambda}/\sigma_{\mathrm{e}}$, $\tilde{\eta}^{\mathrm{sj}} \equiv e^2 \eta^{\mathrm{sj}}/\sigma_{\mathrm{e}}$, $\lambda_\omega \equiv \tilde{\lambda} - \frac{1}{2}\tilde{\eta}^{\mathrm{sj}}$, $\tilde{\eta}_0 \equiv e^2 \eta_0/\sigma_{\mathrm{e}}$, and $\tilde{f}_{\mathrm{AH}} \equiv e^2 f_{\mathrm{AH}}/\sigma_{\mathrm{e}}$. The term $\tilde{\lambda}$ is the AH viscosity force arising from a nondissipative component of the viscosity tensor when the fluid's time-reversal symmetry is broken, which has been intensely discussed for systems under a magnetic field [13,17,36–38]. On the other hand, the term $\lambda_\omega$ is the pressure induced by the vorticity-magnetization coupling, which can also be regarded as an AH contribution to the volume viscosity. The term $\tilde{\eta}^{\mathrm{sj}}$ represents an asymmetric viscosity force arising from $\pi_{ij}^{\mathrm{a}}$. Such a term requires some axial vector such as spin and vorticity to be finite, which, in the present, corresponds to the magnetization vector $\boldsymbol{M}$. Our result indicates an antisymmetric components of the viscosity provides evidence of a side-jump process due to the anomalous velocity.

Using an axial vector $\boldsymbol{a}$, the antisymmetric components of momentum flux density are written as $\pi_{ij}^{\mathrm{a}} = \epsilon_{ijk} a_k$. As read from Eq. (26), the axial vector linear in the spin-orbit interaction, which arises from $\hat{\boldsymbol{M}}$,

$$\boldsymbol{a} = -\frac{4}{3} \tilde{\eta}^{\mathrm{sj}} (\nabla \cdot \boldsymbol{j}) \hat{\boldsymbol{M}} + \tilde{\eta}^{\mathrm{sj}} [\nabla(\hat{\boldsymbol{M}} \cdot \boldsymbol{j}) + (\hat{\boldsymbol{M}} \cdot \nabla) \boldsymbol{j}]. \tag{27}$$

In the contributions to $\boldsymbol{a}$ without $\hat{\boldsymbol{M}}$, there is a term proportional to $\nabla \times \boldsymbol{j}$, which corresponds to a rotational viscosity [22,23,35].

## V. VORTICITY-INDUCED ANOMALOUS HALL EFFECT

Vorticity of flow is usually neglected in bulk transport phenomena in solids as the effect affects only near surfaces or interfaces. In thin film or wires in contrast, the effect would dominate hydrodynamic transport. In the general theory of fluid, the fluid velocity at the interfaces with the container of fluid vanishes and the velocity grows away from the interface. The velocity gradient means the existence of vorticity, $\boldsymbol{\omega} = \nabla \times \boldsymbol{j}$, near the surfaces and interfaces. Our result, Eq. (26), indicates that such surface vortices when coupled to

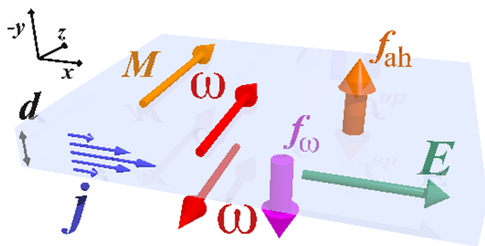


FIG. 3. Schematic picture of the vorticity-induced anomalous Hall effect in a thin film with thickness $d$ with an in-plane magnetization (chosen along the $z$ axis). Applied electric field $E$ along the $x$ direction induces an inhomogeneous fluid velocity $\boldsymbol{v}$ in the thickness direction, resulting in positive and negative vorticities $\boldsymbol{\omega}$ close to the upper and lower plane, respectively. The gradient of the vorticity induces a Hall motive force $f_\omega$ perpendicular to the film, which is in the opposite direction of the conventional anomalous Hall force $f_{\mathrm{AH}}$.

magnetization or magnetic field induces a Hall force or voltage. A suitable setting for observing this effect is a thin film ferromagnet with an in-plane magnetization (Fig. 3). We apply an electric field $\boldsymbol{E}$ perpendicular to the magnetization. In the steady state, the velocity profile in the thickness direction (shown in Fig. 3) calculated from Eq. (26) is [here we ignore higher order of $(\epsilon_F\tau)^{-1}$]

$$j_x(y) = \frac{\sigma_{\mathrm{e}}}{e}E\left[1 - \frac{\cosh(y/l)}{\cosh(d/2l)}\right], \tag{28}$$

where the length scale of the profile $l$ is determined by the viscosity and the electron mean-free path as $l \equiv \sqrt{\sigma_{\mathrm{e}}\tilde{\eta}_0/(ne^2)}$. The velocity variation results in a vorticity, $\boldsymbol{\omega} = \boldsymbol{\nabla}\times\boldsymbol{j}$, positive near the upper plane and negative in the lower plane. The vorticity-magnetization coupling energy $\boldsymbol{\omega}\cdot\hat{\boldsymbol{M}}$ has a gradient in the perpendicular direction, resulting in a vorticity-induced motive force density $\boldsymbol{f}_\omega \equiv \tilde{\lambda}\boldsymbol{\nabla}(\boldsymbol{\omega}\cdot\hat{\boldsymbol{M}})$. Taking account of the elastic lifetime $\tau_{\mathrm{e}}$, the steady perpendicular current density induced by the vorticity is $j_\omega = f_\omega\tau_{\mathrm{e}}/m$. The vorticity due to the current density $j_x$ along the electric field is approximated as $\omega = |\boldsymbol{\nabla}\times\boldsymbol{j}| \simeq j_x/l$ near the surface considering a system thickness $d \gtrsim l$. The gradient of the vorticity is of the order of $\omega/d = j_x/(dl)$. The vorticity-induced current density is therefore $j_\omega = \sigma_\omega E$, where $\sigma_\omega \equiv \frac{\lambda\tau_{\mathrm{e}}}{mdl}$ is the vorticity-induced AH conductivity. In the present model, the order of magnitudes of the coefficient $\lambda$ and the AH conductivity are related by $\lambda \simeq (\epsilon_F\tau_{\mathrm{e}})\sigma_{\mathrm{AH}}$, and thus

$$\sigma_\omega \simeq \sigma_{\mathrm{AH}}\frac{l}{d}. \tag{29}$$

As the present hydrodynamic approach is justified in the regime $d \gtrsim l$, the vorticity-induced Hall effect is at most the same order of magnitude as the conventional AH effect for a thin film of $d \sim l$. Nevertheless, the present vorticity mechanism is a different origin of the Hall effect and could be useful for surface sensitive detection of transport.

The profile of the total Hall electric field calculated from Eq. (26) is [here we ignore the higher order of $(\epsilon_F\tau)^{-1}$]

$$E_{\mathrm{Hall}}(y) = -\left[\frac{f_{\mathrm{AH}}}{n} - \left(2\frac{\lambda}{\eta_0} + \frac{f_{\mathrm{AH}}}{n}\right)\frac{\cosh(y/l)}{\cosh(d/2l)}\right]E, \tag{30}$$

where we included Hall viscosity for generality. The Hall voltage is

$$\begin{aligned} V_{\mathrm{Hall}} &= \int_{-d/2}^{d/2} E_{\mathrm{Hall}}(y)dy \\ &= -\left[\frac{f_{\mathrm{AH}}}{n} - \frac{2l}{d}\left(2\frac{\lambda}{\eta_0} + \frac{f_{\mathrm{ah}}}{n}\right)\tanh(d/2l)\right]Ed. \end{aligned} \tag{31}$$

Here, the first term in the bracket is the conventional one, which is dominant in the bulk limit ($d \to \infty$), whereas the others are the corrections due to the vorticity or velocity gradient, which become important in mesoscopic systems ($d \sim l$). Equation (30) indicates that the bulk and vorticity contributions of the AH effect have opposite signs, resulting in a negative Hall electric field near the boundaries as shown in Fig. 4(a). In the bulk limit, $d \to \infty$, the total Hall voltage [Eq. (31)] reduces to the conventional contribution $\frac{f_{\mathrm{AH}}}{n}Ed$, while vorticity-induced negative contribution dominates in thin systems with $d \sim l$ resulting in $V_{\mathrm{Hall}} \simeq -3\frac{\lambda}{\eta_0}Ed$ [Fig. 4(b)]. The sign change of the Hall voltage by changing the thickness would be useful for experimental identification of the vorticity-induced AH effect. The magnitudes of the two contributions are of the same order in our model; $\lambda/\eta_0 \simeq f_{\mathrm{AH}}/n \simeq (\varepsilon_{\mathrm{so}}/\epsilon_{\mathrm{F}})(M/\epsilon_{\mathrm{F}})$, where $\varepsilon_{\mathrm{so}} \equiv \lambda_{\mathrm{so}}u_{\mathrm{i}}k_{\mathrm{F}}^2$ is the energy scale of the spin-orbit interaction. In general, $\lambda/\eta_0$ and $f_{\mathrm{ah}}/n$ seems to behave independently and could have different orders of magnitude, depending on the details of the systems. However, in our calculations, it is suggested that they always have the same order of magnitude without any fine-tuning. This means that, in many metallic ferromagnets such as Fe and Co, which exhibit the AH effect, it is possible to observe the sign change of the AH voltage by changing the sample thickness to the mean-free path.

Strictly speaking, our results are only applicable to the metallic ferromagnets in the Ohmic regime, but it is expected from the symmetry viewpoint that they are also relevant to the AH systems in the hydrodynamic regime. This conjecture is also supported by the phenomenological arguments in Ref. [23]. One of the possible candidates in the hydrodynamic regime is a 2D monovalent layered metal $PdCoO_2$, which is a nonmagnetic metal in bulk but has been observed to show a surface-magnetization-driven AH effect in ultrathin films [39,40]. In addition, graphene, which is one of the most studied systems in the context of electron hydrodynamics and whose Hall viscosity has already been observed through the nonlocal transport [17], is also considered as an ideal stage to observe the anomalous hydrodynamic flow originating from some magnetic orders. It is well-known that the AH effect arises due to the proximity-induced ferromagnetism when it is coupled to magnetic substrates [41–44] or magnetic nanoparticles [45]. These materials will be intriguing platforms to investigate the hydrodynamic electron transport physics discussed in this paper.

## VI. CONCLUSION

We have derived a hydrodynamic equation for AH electron fluid in the Ohmic regime and found a vorticity-magnetization

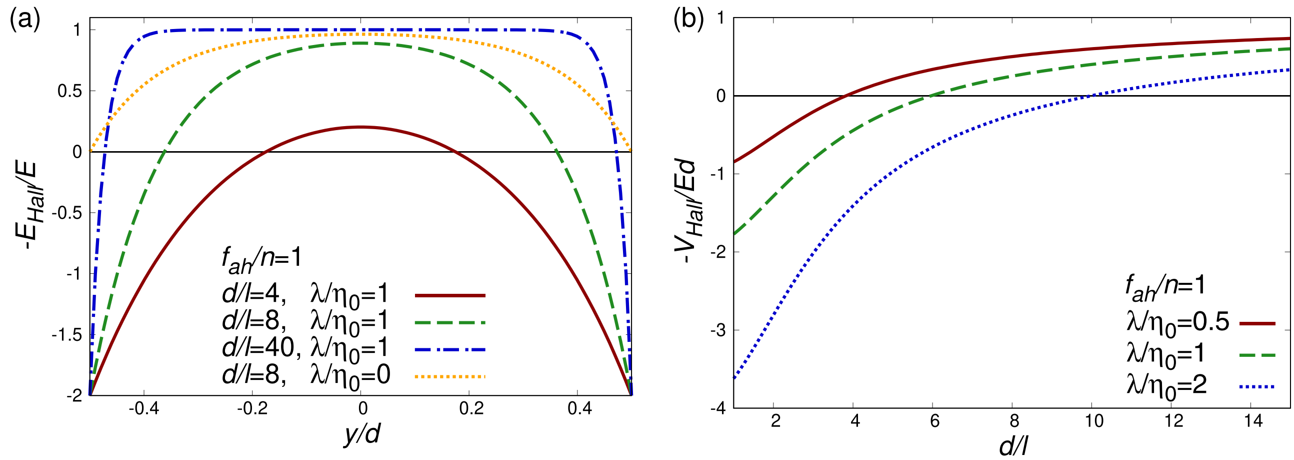


FIG. 4. (a) Spatial distribution of Hall electric field [Eq. (30)]. (b) System thickness dependence of the total Hall voltage [Eq. (31)], plotted for different value for $\lambda/\eta_0$.

coupling contribution in the momentum flux density. The coupling induces a vorticity-induced additional AH effect in the opposite direction as the conventional AH effect, suggesting a sign reversal of AH voltage in thin systems. Furthermore, we can also consider nonlocal measurements in the so-called vicinity geometry [8,46] as another possible setup to detect the effect of the vorticity-magnetization coupling and the Hall viscosity. Actually, in the geometry, viscous effects in the nonlocal transport, including Hall viscosity effects, has already been observed in several materials [9,17,47,48].

For vorticity to arise, the existence of a boundary is generally essential, as the vorticity is parity invariant, while linear driving field is odd. A inversion symmetry breaking due to the boundary is thus necessary.

Spin chirality $\boldsymbol{\chi}$ has been pointed out to be an another origin of the AH effect. The study of the perturbative regime in Ref. [49] is straightforwardly extended to the calculation of the momentum flux density, resulting in a coupling $\boldsymbol{\chi}\cdot\boldsymbol{\omega}$.

## ACKNOWLEDGMENTS

This study was supported by a Grant-in-Aid for Scientific Research (B) (No. 17H02929 and No. 21H01034) from the Japan Society for the Promotion of Science and JSPS KAKENHI (Grant No. 20J22612).

## APPENDIX A: NORMAL VISCOSITY OF OHMIC FLUID

Here we calculate the normal viscosity constant in the present Ohmic fluid for consistency. The normal contribution to the momentum flux density is

$$\pi^{(0)}_{ij}(\boldsymbol{r},t)\equiv -i\frac{1}{m}\mathrm{tr}[\hat{p}_i\hat{p}_jG^<(\boldsymbol{r},t,\boldsymbol{r},t)], \tag{A1}$$

where the Green's function here is without the spin-orbit interaction. Taking account of the static external electric field, described by a gauge field $\boldsymbol{A}$ as $\boldsymbol{E}=-\dot{\boldsymbol{A}}$, to the linear order, it reads in the Fourier representation $\pi^{(0)}_{ij}(\boldsymbol{q},\Omega)=\int d^3r\int dt\pi^{(0)}_{ij}(\boldsymbol{r},t)e^{-i\boldsymbol{q}\cdot\boldsymbol{r}}e^{i\Omega t}$,

$$\pi^{(0)}_{ij}(\boldsymbol{q})=i\frac{e}{m^2}\frac{1}{V}\sum_{\boldsymbol{k}}\int\frac{d\omega}{2\pi}\lim_{\Omega\to 0}k_ik_jk_k[G_{\boldsymbol{k}+\frac{\boldsymbol{q}}{2},\omega+\Omega}G_{\boldsymbol{k}-\frac{\boldsymbol{q}}{2},\omega}]^<A_k(\boldsymbol{q},\Omega)\equiv\pi^{(0)}_{ijk}(\boldsymbol{q})eE_k(\boldsymbol{q}), \tag{A2}$$

where $\omega$ and $\boldsymbol{k}$, $\Omega$ and $\boldsymbol{q}$ denote the angular frequency and wave vector of electron and external field, respectively. Here we neglect the diffusive contribution as it affects only the nonequilibrium state. The response function is

$$\pi^{(0)}_{ijk}(\boldsymbol{q})\equiv\frac{1}{m^2}\frac{1}{V}\sum_{\boldsymbol{k}}\int\frac{d\omega}{2\pi}\lim_{\Omega\to 0}\frac{1}{\Omega}k_ik_jk_k[G_{\boldsymbol{k}+\frac{\boldsymbol{q}}{2},\omega+\Omega}G_{\boldsymbol{k}-\frac{\boldsymbol{q}}{2},\omega}]^<. \tag{A3}$$

The lesser component is decomposed into the retarded and advanced Green's functions as

$$[G_{\boldsymbol{k}+\frac{\boldsymbol{q}}{2},\omega+\Omega}G_{\boldsymbol{k}-\frac{\boldsymbol{q}}{2},\omega}]^<=(f_\omega-f_{\omega+\Omega})G^{\mathrm{r}}_{\boldsymbol{k}+\frac{\boldsymbol{q}}{2},\omega+\Omega}G^{\mathrm{a}}_{\boldsymbol{k}-\frac{\boldsymbol{q}}{2},\omega}-f_\omega G^{\mathrm{r}}_{\boldsymbol{k}+\frac{\boldsymbol{q}}{2},\omega+\Omega}G^{\mathrm{r}}_{\boldsymbol{k}-\frac{\boldsymbol{q}}{2},\omega}+f_{\omega+\Omega}G^{\mathrm{a}}_{\boldsymbol{k}+\frac{\boldsymbol{q}}{2},\omega+\Omega}G^{\mathrm{a}}_{\boldsymbol{k}-\frac{\boldsymbol{q}}{2},\omega}, \tag{A4}$$

where $f_\omega=[e^{\beta\omega}+1]^{-1}$ is the Fermi distribution function. Expanding the expression with respect to $\Omega$, we obtain

$$\begin{aligned}[G_{\boldsymbol{k}+\frac{\boldsymbol{q}}{2},\omega+\Omega}G_{\boldsymbol{k}-\frac{\boldsymbol{q}}{2},\omega}]^<=\;&f_\omega\big[G^{\mathrm{a}}_{\boldsymbol{k}+\frac{\boldsymbol{q}}{2},\omega}G^{\mathrm{a}}_{\boldsymbol{k}-\frac{\boldsymbol{q}}{2},\omega}-G^{\mathrm{r}}_{\boldsymbol{k}+\frac{\boldsymbol{q}}{2},\omega}G^{\mathrm{r}}_{\boldsymbol{k}-\frac{\boldsymbol{q}}{2},\omega}\big]\\&+\Omega f'_\omega\left[-G^{\mathrm{r}}_{\boldsymbol{k}+\frac{\boldsymbol{q}}{2},\omega}G^{\mathrm{a}}_{\boldsymbol{k}-\frac{\boldsymbol{q}}{2},\omega}+\frac{1}{2}\big(G^{\mathrm{a}}_{\boldsymbol{k}+\frac{\boldsymbol{q}}{2},\omega}G^{\mathrm{a}}_{\boldsymbol{k}-\frac{\boldsymbol{q}}{2},\omega}+G^{\mathrm{r}}_{\boldsymbol{k}+\frac{\boldsymbol{q}}{2},\omega}G^{\mathrm{r}}_{\boldsymbol{k}-\frac{\boldsymbol{q}}{2},\omega}\big)\right]\\&+\frac{\Omega}{2}f_\omega\big[-G^{\mathrm{a}}_{\boldsymbol{k}+\frac{\boldsymbol{q}}{2},\omega}\overleftrightarrow{\partial_\omega}G^{\mathrm{a}}_{\boldsymbol{k}-\frac{\boldsymbol{q}}{2},\omega}+G^{\mathrm{r}}_{\boldsymbol{k}+\frac{\boldsymbol{q}}{2},\omega}\overleftrightarrow{\partial_\omega}G^{\mathrm{r}}_{\boldsymbol{k}-\frac{\boldsymbol{q}}{2},\omega}\big].\end{aligned} \tag{A5}$$

The contribution of the order of $\Omega^0$ turns out to cancel the contribution from the anomalous velocity $\delta v$. The last term of the right-hand side of Eq. (A5) is smaller than the main contribution, the second term, by a factor of $(\epsilon_F \tau_e)^{-1}$ and is neglected. The response function is, therefore, using $f'(\omega) = -\delta(\omega)$ at low temperatures,

$$\pi^{(0)}_{ijk}(\boldsymbol{q}) \equiv \frac{1}{m^2}\frac{1}{V}\sum_{\boldsymbol{k}}\int \frac{d\omega}{2\pi} f'(\omega) k_i k_j k_k \left[-G^{\rm r}_{\boldsymbol{k}+\frac{\boldsymbol{q}}{2},\omega} G^{\rm a}_{\boldsymbol{k}-\frac{\boldsymbol{q}}{2},\omega} + \frac{1}{2}\left(G^{\rm a}_{\boldsymbol{k}+\frac{\boldsymbol{q}}{2},\omega} G^{\rm a}_{\boldsymbol{k}-\frac{\boldsymbol{q}}{2},\omega} + G^{\rm r}_{\boldsymbol{k}+\frac{\boldsymbol{q}}{2},\omega} G^{\rm r}_{\boldsymbol{k}-\frac{\boldsymbol{q}}{2},\omega}\right)\right]$$
$$= -\frac{1}{2\pi}\frac{1}{m^2}\frac{1}{V}\sum_{\boldsymbol{k}} k_i k_j k_k \left[-G^{\rm r}_{\boldsymbol{k}+\frac{\boldsymbol{q}}{2},\omega} G^{\rm a}_{\boldsymbol{k}-\frac{\boldsymbol{q}}{2},\omega} + \frac{1}{2}\left(G^{\rm a}_{\boldsymbol{k}+\frac{\boldsymbol{q}}{2},\omega} G^{\rm a}_{\boldsymbol{k}-\frac{\boldsymbol{q}}{2},\omega} + G^{\rm r}_{\boldsymbol{k}+\frac{\boldsymbol{q}}{2},\omega} G^{\rm r}_{\boldsymbol{k}-\frac{\boldsymbol{q}}{2},\omega}\right)\right], \tag{A6}$$

where $G_{\boldsymbol{k}} \equiv G_{\boldsymbol{k},\omega=0}$. Expanding with respect to $q$ and using rotational symmetry in $\boldsymbol{k}$, we obtain

$$\pi^{(0)}_{ijk}(\boldsymbol{q}) = \frac{-1}{4\pi V}\frac{iq_l}{m^3\tau_e}\sum_{\boldsymbol{k}} k_i k_j k_k k_l \left|G^{\rm r}_{\boldsymbol{k}}\right|^4$$
$$= -\eta_0 i[\delta_{ij}q_k + \delta_{ik}q_j + \delta_{jk}q_i], \tag{A7}$$

where $\eta_0 \equiv \frac{\nu k_F{}^4 \tau_e^2}{15 m^3}$ is a normal viscosity constant. Using $\nu \sim \epsilon_F$, it is $\eta_0 \simeq l_e^2$, where $l_e \equiv \frac{k_F}{m}\tau_e$ is the elastic mean-free path. Including the external field,

$$\pi^{(0)}_{ij} = -e\eta_0[\delta_{ij}\nabla\cdot\boldsymbol{E} + \nabla_i E_j + \nabla_j E_i], \tag{A8}$$

the contribution to the time-derivative of momentum density is

$$-\nabla_j \pi^{(0)}_{ij} = e\eta_0[2\nabla(\nabla\cdot\boldsymbol{E}) + \nabla^2\boldsymbol{E}]. \tag{A9}$$

### APPENDIX B: ANOMALOUS HALL FORCE OPERATOR

This section shows the derivation of the AH force operator $f_i^{\rm so}$ and the momentum flux operator from spin-orbit interaction $\pi^{\rm so}_{ij}$. The commutator in Eq. (8) is

$$i[H_{\rm so}, c^\dagger \hat{p}_{\rm i} c] = \frac{-i}{4}\lambda_{\rm so}\int d^3r' \epsilon_{jkl}\nabla'_j u_{\rm i}(\boldsymbol{r}')[c^\dagger(\boldsymbol{r}')\sigma_l \nabla'_k c(\boldsymbol{r}')$$
$$- {\rm H.c.}, c^\dagger \nabla_i c - {\rm H.c.}]$$
$$= \frac{-i}{4}\lambda_{\rm so}\int d^3r' \epsilon_{jkl}\nabla'_j u_{\rm i}(\boldsymbol{r}')[\{c^\dagger(\boldsymbol{r}')\sigma_l$$
$$\times \nabla'_k \delta(\boldsymbol{r}'-\boldsymbol{r})\nabla_i c - c^\dagger \sigma_l \nabla_i \delta(\boldsymbol{r}'-\boldsymbol{r})\, \nabla'_k c(\boldsymbol{r}')\}$$
$$- {\rm H.c.} + \{-c^\dagger(\boldsymbol{r}')\sigma_l \nabla_i \nabla'_k \delta(\boldsymbol{r}'-\boldsymbol{r})c$$
$$+ \nabla_i c^\dagger \sigma_l \delta(\boldsymbol{r}'-\boldsymbol{r})\nabla'_k c(\boldsymbol{r}')\} - {\rm H.c.}]. \tag{B1}$$

Writing derivatives of the $\delta$ functions with respect to $\boldsymbol{r}$ ($\nabla$) by derivatives with respect to $\boldsymbol{r}'$ ($\nabla'$) and using integral by parts, we obtain

$$i[H_{\rm so}, c^\dagger \hat{p}_{\rm i} c] = \frac{i}{2}\lambda_{\rm so}\epsilon_{jkl}[\nabla_k\{\nabla_j u_{\rm i}(c^\dagger \sigma_l \nabla_i c - {\rm H.c.})\}$$
$$+ \nabla_i \nabla_j u_{\rm i}(c^\dagger \sigma_l \nabla_k c - {\rm H.c.})], \tag{B2}$$

namely,

$$\pi^{\rm so}_{ij} = \frac{i}{2}\lambda_{\rm so}\epsilon_{jkl}\nabla_k u_{\rm i}(c^\dagger \sigma_l \nabla_i c - {\rm H.c.}) \tag{B3}$$

$$f^{\rm so}_i = \frac{i}{2}\lambda_{\rm so}\epsilon_{jkl}\nabla_i \nabla_j u_{\rm i}(c^\dagger \sigma_l \nabla_k c - {\rm H.c.}). \tag{B4}$$

[1] M. Matsuo, J. Ieda, E. Saitoh, and S. Maekawa, Effects of Mechanical Rotation on Spin Currents, Phys. Rev. Lett. **106**, 076601 (2011).
[2] M. Matsuo, Y. Ohnuma, and S. Maekawa, Theory of spin hydrodynamic generation, Phys. Rev. B **96**, 020401(R) (2017).
[3] M. Dyakonov and V. Perel, Current-induced spin orientation of electrons in semiconductors, Phys. Lett. A **35**, 459 (1971).
[4] J. E. Hirsch, Spin Hall Effect, Phys. Rev. Lett. **83**, 1834 (1999).
[5] G. Tatara, Spin correlation function theory of spin-charge conversion effects, Phys. Rev. B **98**, 174422 (2018).
[6] A. Lucas and K. C. Fong, Hydrodynamics of electrons in graphene, J. Phys.: Condens. Matter **30**, 053001 (2018).
[7] M. Polini and A. K. Geim, Viscous electron fluids, Phys. Today **73**, 28 (2020).
[8] I. Torre, A. Tomadin, A. K. Geim, and M. Polini, Nonlocal transport and the hydrodynamic shear viscosity in graphene, Phys. Rev. B **92**, 165433 (2015).
[9] D. A. Bandurin, I. Torre, R. K. Kumar, M. Ben Shalom, A. Tomadin, A. Principi, G. H. Auton, E. Khestanova, K. S. Novoselov, I. V. Grigorieva, L. A. Ponomarenko, A. K. Geim, and M. Polini, Negative local resistance caused by viscous electron backflow in graphene, Science **351**, 1055 (2016).
[10] L. Levitov and G. Falkovich, Electron viscosity, current vortices and negative nonlocal resistance in graphene, Nat. Phys. **12**, 672 (2016).
[11] D. A. Bandurin, A. V. Shytov, L. S. Levitov, R. K. Kumar, A. I. Berdyugin, M. Ben Shalom, I. V. Grigorieva, A. K. Geim, and G. Falkovich, Fluidity onset in graphene, Nat. Commun. **9**, 4533 (2018).
[12] P. S. Alekseev, Negative Magnetoresistance in Viscous Flow of Two-Dimensional Electrons, Phys. Rev. Lett. **117**, 166601 (2016).
[13] T. Scaffidi, N. Nandi, B. Schmidt, A. P. Mackenzie, and J. E. Moore, Hydrodynamic Electron Flow and Hall Viscosity, Phys. Rev. Lett. **118**, 226601 (2017).
[14] F. M. D. Pellegrino, I. Torre, and M. Polini, Nonlocal transport and the Hall viscosity of two-dimensional hydrodynamic electron liquids, Phys. Rev. B **96**, 195401 (2017).

[15] P. J. W. Moll, P. Kushwaha, N. Nandi, B. Schmidt, and A. P. Mackenzie, Evidence for hydrodynamic electron flow in $PdCoO_2$, Science **351**, 1061 (2016).

[16] J. Gooth, F. Menges, C. Shekhar, V. Süß, N. Kumar, Y. Sun, U. Drechsler, R. Zierold, C. Felser, and B. Gotsmann, Thermal and electrical signatures of a hydrodynamic electron fluid in tungsten diphosphide, Nat. Commun. **9**, 4093 (2018).

[17] A. I. Berdyugin, S. G. Xu, F. M. D. Pellegrino, R. Krishna Kumar, A. Principi, I. Torre, M. Ben Shalom, T. Taniguchi, K. Watanabe, I. V. Grigorieva, M. Polini, A. K. Geim, and D. A. Bandurin, Measuring Hall viscosity of graphene's electron fluid, Science **364**, 162 (2019).

[18] M. Matsuo, D. A. Bandurin, Y. Ohnuma, Y. Tsutsumi, and S. Maekawa, Spin hydrodynamic generation in graphene, arXiv:2005.01493.

[19] R. Toshio, K. Takasan, and N. Kawakami, Anomalous hydrodynamic transport in interacting noncentrosymmetric metals, Phys. Rev. Research **2**, 032021(R) (2020).

[20] A. Shitade, K. Mameda, and T. Hayata, Chiral vortical effect in relativistic and nonrelativistic systems, Phys. Rev. B **102**, 205201 (2020).

[21] H. Funaki and G. Tatara, Hydrodynamic theory of chiral angular momentum generation in metals, Phys. Rev. Research **3**, 023160 (2021).

[22] S. R. de Groot and P. Mazur, *Non-equilibrium Thermodynamics* (North-Holland, Amsterdam, 1962; Dover, New York, 1984).

[23] R. F. Snider and K. S. Lewchuk, Irreversible thermodynamics of a fluid system with spin, J. Chem. Phys. **46**, 3163 (1967).

[24] R. Gurzhi, Minimum of resistance in impurity-free conductors, JETP **17**, 521 (1963) [ZhETF **44**, 771 (1963)].

[25] J. Crossno, J. K. Shi, K. Wang, X. Liu, A. Harzheim, A. Lucas, S. Sachdev, P. Kim, T. Taniguchi, K. Watanabe, T. A. Ohki, and K. C. Fong, Observation of the Dirac fluid and the breakdown of the Wiedemann-Franz law in graphene, Science **351**, 1058 (2016).

[26] R. K. Kumar, D. Bandurin, F. Pellegrino, Y. Cao, A. Principi, H. Guo, G. Auton, M. B. Shalom, L. A. Ponomarenko, G. Falkovich *et al.*, Superballistic flow of viscous electron fluid through graphene constrictions, Nat. Phys. **13**, 1182 (2017).

[27] J. A. Sulpizio, L. Ella, A. Rozen, J. Birkbeck, D. J. Perello, D. Dutta, M. Ben-Shalom, T. Taniguchi, K. Watanabe, T. Holder, R. Queiroz, A. Principi, A. Stern, T. Scaffidi, A. K. Geim, and S. Ilani, Visualizing Poiseuille flow of hydrodynamic electrons, Nature **576**, 75 (2019).

[28] L. W. Molenkamp and M. J. M. de Jong, Electron-electron-scattering-induced size effects in a two-dimensional wire, Phys. Rev. B **49**, 5038 (1994).

[29] M. J. M. de Jong and L. W. Molenkamp, Hydrodynamic electron flow in high-mobility wires, Phys. Rev. B **51**, 13389 (1995).

[30] U. Vool, A. Hamo, G. Varnavides, Y. Wang, T. X. Zhou, N. Kumar, Y. Dovzhenko, Z. Qiu, C. A. C. Garcia, A. T. Pierce, J. Gooth, P. Anikeeva, C. Felser, P. Narang, and A. Yacoby, Imaging phonon-mediated hydrodynamic flow in $WTe_2$ with cryogenic quantum magnetometry, arXiv:2009.04477.

[31] N. Kumar, Y. Sun, M. Nicklas, S. J. Watzman, O. Young, I. Leermakers, J. Hornung, J. Klotz, J. Gooth, K. Manna, V. Süß, S. N. Guin, T. Förster, M. Schmidt, L. Muechler, B. Yan, P. Werner, W. Schnelle, U. Zeitler, J. Wosnitza, S. S. P. Parkin, C. Felser, and C. Shekhar, Extremely high conductivity observed in the triple point topological metal mop, Nat. Commun. **10**, 2475 (2019).

[32] A. Jaoui, B. Fauqué, and K. Behnia, Thermal resistivity and hydrodynamics of the degenerate electron fluid in antimony, Nat. Commun. **12**, 195 (2021).

[33] C. woo Cho, P. Wang, F. Tang, S. Park, M. He, R. Lortz, G. Gu, and L. Zhang, Observation of hydrodynamic-like behavior in 3D Dirac semimetal $ZrTe_5$, arXiv:2011.01597.

[34] V. K. Dugaev, A. Crépieux, and P. Bruno, Localization corrections to the anomalous Hall effect in a ferromagnet, Phys. Rev. B **64**, 104411 (2001).

[35] R. J. Doornenbal, M. Polini, and R. A. Duine, Spin–vorticity coupling in viscous electron fluids, J. Phys.: Mater. **2**, 015006 (2019).

[36] J. E. Avron, Odd viscosity, J. Stat. Phys. **92**, 543 (1998).

[37] N. Read, Non-Abelian adiabatic statistics and Hall viscosity in quantum Hall states and $p_x + ip_y$ paired superfluids, Phys. Rev. B **79**, 045308 (2009).

[38] C. Hoyos and D. T. Son, Hall Viscosity and Electromagnetic Response, Phys. Rev. Lett. **108**, 066805 (2012).

[39] K. Kim, H. C. Choi, and B. I. Min, Fermi surface and surface electronic structure of delafossite $PdCoO_2$, Phys. Rev. B **80**, 035116 (2009).

[40] T. Harada, K. Sugawara, K. Fujiwara, M. Kitamura, S. Ito, T. Nojima, K. Horiba, H. Kumigashira, T. Takahashi, T. Sato, and A. Tsukazaki, Anomalous Hall effect at the spontaneously electron-doped polar surface of $PdCoO_2$ ultrathin films, Phys. Rev. Research **2**, 013282 (2020).

[41] Z. Wang, C. Tang, R. Sachs, Y. Barlas, and J. Shi, Proximity-induced Ferromagnetism in Graphene Revealed by the Anomalous Hall Effect, Phys. Rev. Lett. **114**, 016603 (2015).

[42] C. Tang, B. Cheng, M. Aldosary, Z. Wang, Z. Jiang, K. Watanabe, T. Taniguchi, M. Bockrath, and J. Shi, Approaching quantum anomalous Hall effect in proximity-coupled YIG/graphene/h-BN sandwich structure, APL Mater. **6**, 026401 (2018).

[43] D. V. Averyanov, I. S. Sokolov, A. M. Tokmachev, O. E. Parfenov, I. A. Karateev, A. N. Taldenkov, and V. G. Storchak, High-temperature magnetism in graphene induced by proximity to EuO, ACS Appl. Mater. Interfaces **10**, 20767 (2018).

[44] H.-D. Song, P.-F. Zhu, J. Fang, Z. Zhou, H. Yang, K. Wang, J. Li, D. Yu, Z. Wei, and Z.-M. Liao, Anomalous Hall effect in graphene coupled to a layered magnetic semiconductor, Phys. Rev. B **103**, 125304 (2021).

[45] G. Song, M. Ranjbar, D. R. Daughton, and R. A. Kiehl, Nanoparticle-induced anomalous Hall effect in graphene, Nano Lett. **19**, 7112 (2019).

[46] F. M. D. Pellegrino, I. Torre, A. K. Geim, and M. Polini, Electron hydrodynamics dilemma: Whirlpools or no whirlpools, Phys. Rev. B **94**, 155414 (2016).

[47] A. D. Levin, G. M. Gusev, E. V. Levinson, Z. D. Kvon, and A. K. Bakarov, Vorticity-induced negative nonlocal resistance in a viscous two-dimensional electron system, Phys. Rev. B **97**, 245308 (2018).

[48] G. M. Gusev, A. D. Levin, E. V. Levinson, and A. K. Bakarov, Viscous transport and Hall viscosity in a two-dimensional electron system, Phys. Rev. B **98**, 161303(R) (2018).

[49] G. Tatara and H. Kawamura, Chirality-driven anomalous Hall effect in weak coupling regime, J. Phys. Soc. Jpn. **71**, 2613 (2002).